ECS Journal of Solid State
Science and Technology

A DLTS Perspective on Electrically Active Defects in Plated Crystalline Silicon n^+p Solar Cells

A DLTS Perspective on Electrically Active Defects in Plated Crystalline Silicon n^+p Solar Cells

E. Simoen,[1,2,*,z] C. Dang,[1,3,4] R. Labie,[1] and J. Poortmans[1,3,4]

[1]*Imec, 3001 Leuven, Belgium*
[2]*Ghent University, 9000 Gent, Belgium*
[3]*KU Leuven, Department Elektrotechniek - ESAT, 3001 Leuven, Belgium*
[4]*UHasselt, 3590 Hasselt, Belgium*

Laser ablation (LA) has been compared with standard wet etching for contact opening in crystalline silicon n^+p solar cells, from a perspective of electrically active defects, assessed by Deep-Level Transient Spectroscopy (DLTS). Copper metallization is employed, including a plated nickel diffusion barrier. It is shown that a hole trap around 0.17 eV above the valence band is systematically present in the depletion region of the junctions, irrespective of the contact opening method. This level could correspond with the substitutional nickel donor level in silicon and indicates that Ni in-diffusion occurs during the contact processing. No clear evidence for the presence of electrically active copper has been found. In addition, two other hole traps H2 and H3, belonging to point defects, have been observed after wet etching and standard LA, while for the highest laser power (hard LA) a broad band develops around 175 K, which is believed to be associated with dislocations, penetrating the p-type base region. Evidence will also be given for the impurity decoration of the dislocations, which enhances their electrical activity.
 [DOI: 10.1149/2.0111911jss]

Manuscript submitted July 25, 2019; revised manuscript received October 22, 2019. Published November 1, 2019. This was Paper 1190 presented at the Cancun, Mexico, Meeting of the Society, September 30–October 4, 2018.

Cost reduction is one of the major driving forces in the technology development of silicon solar cells. This explains the current interest in the introduction of a copper-based metallization, replacing more expensive Ag contacts.[1–3] The implementation of copper interconnects in Complementary Metal-Oxide-Semiconductor (CMOS) technology has elucidated that there exist several yield and reliability issues.[4] From a perspective of solar cell performance, one should in the first instance be concerned with the presence of copper in the depletion and the neutral base region, which can degrade the generation and recombination lifetime, respectively.

Interstitial copper (Cu_i) is one of the fastest diffusors in silicon, so that it can penetrate deep in the substrate at reasonable time scales, even at room temperature.[5] In dissolved form, i.e., as individual atom or in small defect pairs/complexes, its impact on the recombination lifetime[6–10] and solar cell performance[11–13] is rather limited. This is related to the fact that the electrically active substitutional state forms only a fraction of the total solid solubility, compared with the dominant mobile Cu_i.[5] The latter is a positively charged donor, with a level close to the conduction band. At room temperature, copper will be in supersaturation and the interstitials tend to precipitate at the surface or at internal sinks, given their high diffusivity. In the former case, the presence of Cu at the Si/SiO_2 interface will increase the surface recombination velocity by creating a higher density of interface states.[14] In precipitated form, the impact of copper on the recombination lifetime is much more pronounced.[15–17] This is opposite to the behavior of iron, another well-known transition-metal impurity in silicon.[18] It is believed that copper precipitation is the origin of the so-called copper-related light-induced degradation (Cu-LID) of the minority carrier lifetime τ.[19] Therefore, to preserve the efficiency in crystalline-silicon solar cells with copper metallization, one should avoid its presence in the base region.

In order to prevent the in-diffusion of copper in the underlying silicon substrate, a diffusion barrier, like, e.g., a thin nickel layer is usually applied.[1–3] However, Ni behaves rather similar to copper, with a solid solubility governed by the fast diffusing interstitial species and a small fraction of electrically active substitutional nickel (Ni_s).[20] This implies that the impact on the bulk recombination lifetime is rather moderate.[21–24] At the same time, the donor level of interstitial nickel (Ni_i) is expected to be close to or even inside the valence band, so that it will be always in the neutral charge state in silicon. Again, nickel will have a strong tendency to precipitate.[25] When present in a silicon p-n junction, for example as a consequence of a too aggressive nickel silicidation step, nickel precipitates will degrade the reverse dark current,[26,27] an undesirable feature for optimal solar cell performance.

Opening of the passivation layer for contact formation by laser ablation (LA), enables a better controll for narrower line features, compared with standard wet etching. In addition, it can reduce the process complexity and cost.[28] Drawback is that when a too high laser power is applied, extended defects (dislocations) are formed[28–30] which may penetrate from the n^+ emitter into the p-type silicon base region. It has been shown that these dislocations are electrically active[28] and become even more so after solar cell ageing,[31] especially when decorated with transition metal atoms.

In this work, potential issues with defect fomation associated with laser ablation and metal plating will be studied relying on Deep-Level Transient Spectroscopy (DLTS)[32,33] on n^+-p junction diodes. Electrically active defects in the p-type base depletion region have been investigated as a function of the LA power conditions (hard versus standard); as a reference, solar cells fabricated with a wet-etch opening of the contact areas are studied as well. It is shown that while there is evidence for the presence of nickel in the p-type base, no measurable electrically active copper has been found. For hard LA conditions, the presence of dislocations in the depletion region is shown, which could form an issue with respect to the reliability of the solar cells.[31]

Processing and Measurement Details

P-doped n^+-type emitters have been fabricated by $POCl_3$ diffusion into 1–3 Ωcm p-type Czochralski silicon substrates. Passivation of the textured solar cells has been achieved by Plasma-Enhanced Chemical Vapor Deposition (PECVD) of a SiN_x:H layer on top of SiO_2. The ∼100 nm dielectric layer at the front was opened by ps UltraViolet (UV)-laser ablation (355 nm wavelength), using a low (0.72 J/cm^2), standard or high fluence (1.08 J/cm^2) (hard LA). The laser spot was 12 μm, with 50% overlap between the adjacent spots. The contact opening size was 1.5 × 1.5 mm^2. This was compared with contact hole opening by wet etching (WE) to remove the 100 nm SiN_x/SiO_2 passivation layer. After contact opening, approximately 1 μm of nickel was deposited by light-induced plating, followed by 8 to 10 μm of electroplated copper. More details of the processing have been previously reported.[30,34,35]

*Electrochemical Society Fellow.
[z]E-mail: eddy.simoen@imec.be

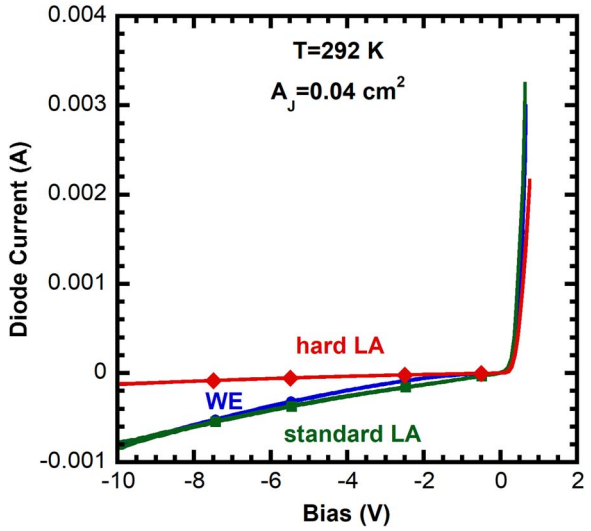

Figure 1. I-V characteristics for a wet-etched, a standard and a hard LA n^+p junction at 292 K.

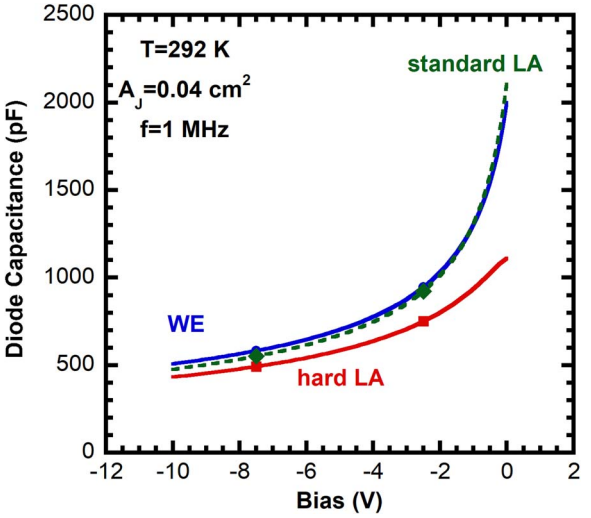

Figure 2. C-V characteristics for a wet-etched, a standard and a hard LA n^+p junction at 292 K. The frequency of the ac modulation signal of 30 mV is 1 MHz.

Diodes with area A_J of 2mm × 2mm were laser-cut from the finished solar cells for DLTS analysis. In this way, an n^+p junction is obtained with a maximum capacitance below the system limit of 3 nF. Before cooling the sample in a liquid-nitrogen flow cryostat, Current-Voltage (I-V) and Capacitance-Voltage (C-V) measurements have been performed at room temperature (RT), the latter at a fixed frequency of 1 MHz. The doping density N_{dop} and profile versus depletion depth W have been derived from a C^{-2} versus V_R plot. Hereby is the depletion width given by:

$$W(V_R) = \varepsilon_0 \varepsilon_{Si} A_J C(V_R) \quad [1]$$

with ε_0 the permittivity of vacuum and ε_{Si} the dielectric constant of silicon. DLTS has been executed using a Fast-Fourier Transform (FFT) system from PhysTech. Temperature (T-) scans have been performed at different bias pulses from a reverse bias V_R to a pulse bias V_P, for different durations t_p, ranging from 10 ns to 1 s, using the fast pulse mode. The latter type of measurements has been used to derive the trap filling kinetics. The pulse period was t_w. Typical values of W for a V_R from 0 V to −10 V are in the range of 0.5 to 1 μm, which also defines the region where the deep level information in DLTS is coming from. Arrhenius plots have been derived by calculating numerically the spectra for different combinations of the Fourier coefficients, varying the hole emission time constant (τ) window and linear fitting the obtained τT^2 versus $1/k_BT$ data points (k_B Boltzmann's constant).

Results and Discussion

First, the results of the basic diode characterization (I-V; C-V; doping profile) will be discussed, followed by a description of the DLTS results.

Basic n^+p diode characteristics.—According to Fig. 1, reasonable I-V characteristics have been obtained for the wet-etched (WE) and LA n^+p junctions at room temperature. It should be remarked here that the edges of the wafer-cut diodes have not been passivated. This could cause significant additional perimeter leakage, assisted by the dangling bonds/damage at these sidewalls. It may explain the fairly high dark current for the WE and standard LA diodes at $V_R = -10$ V, compared with the hard LA diode. In fact, for the finished solar cells the leakage current, dominated by carrier generation in the bulk depletion region, is highest for hard LA, due to the presence of dislocations in the p-type base region.[34,35] At the same time, the reverse current was found to be thermally activated, reducing at lower T. In this way, the DLTS measurements will not be affected too much by the leakage current.

The corresponding C-V curves at 1 MHz are represented in Fig. 2. For all reported junctions, a B doping density in the range of 1.5 to 2.2×10^{16} cm^{-3} is derived in Fig. 3, with a profile decaying slightly at larger depths. The differences between the diodes fall within the estimated 10% accuracy of the C-V measurements and are consistent with the specified resistivity of the starting p-type wafers. In addition, the measurement range for deep levels in DLTS derived from Fig. 3 is approximately between 0.2 μm and 1 μm below the junction, in the p-type base.

Deep levels in the p-type base.—The spectra for the wet etched sample in Fig. 4 exhibit two main hole traps in the p-type base layer: a peak H1 at about 80 K and another one H2 at ∼150 K. A third minor peak H3 occurs close to RT (∼250 K). The activation energy E_A of the first trap amounts to 0.17 eV and a hole capture cross section σ_p of $\sim 7 \times 10^{-15}$ cm^2 (Fig. 5). As argued previously,[34,35] this level most likely originates from the substitutional nickel ($Ni_s^{+/0}$) donor level at E_V+0.160 eV[36] (E_V, the top of the valence band). Another candidate is the $Cu_s^{+/0}$ donor level at E_V+0.207 eV.[37] However, the

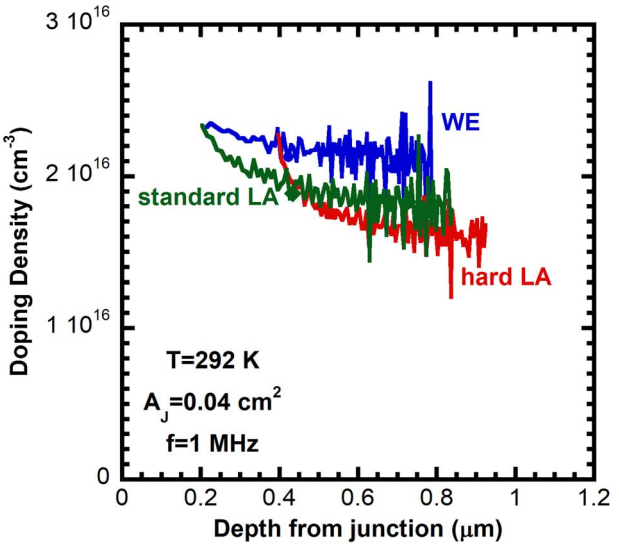

Figure 3. Doping concentration profile for a wet-etched, a standard and a hard LA n^+p junction at 292 K.

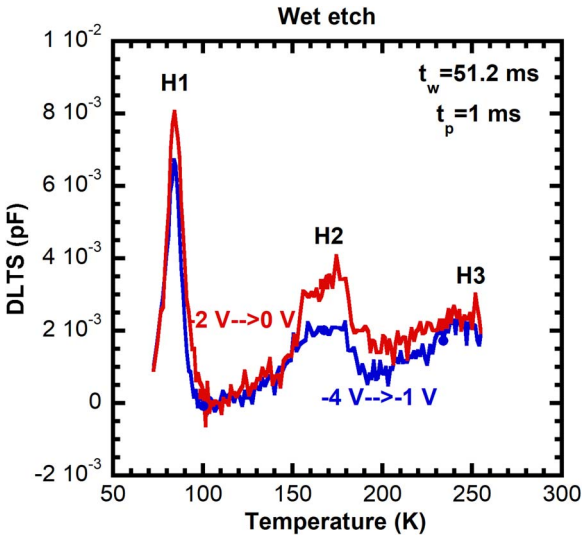

Figure 4. DLT-spectra for different bias pulses, using a sampling period t_w = 51.2 ms and a pulse duration t_p = 1 ms for a wet-etched n^+p diode.

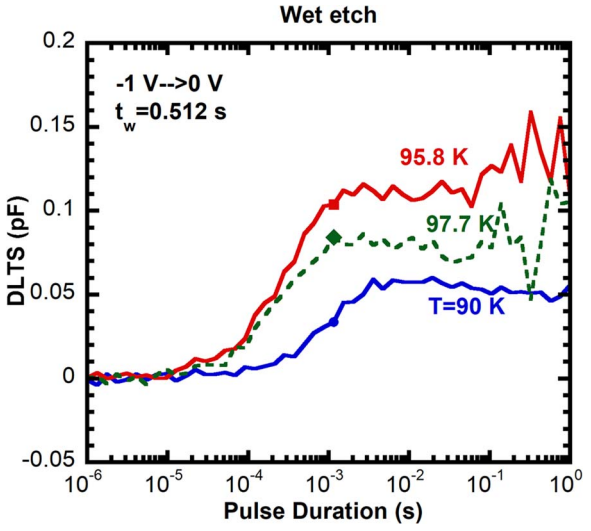

Figure 6. DLTS amplitude versus pulse duration for the H1 peak in a wet etched n^+p junction, corresponding with different measurement temperatures and a sampling period t_w = 0.512 s. The pulse was from −1 V to 0 V.

agreement of the measured Arrhenius plot is considerably better for the Ni_s level. This suggests that there is some Ni in-diffusion in the silicon wafer, yielding concentrations in the range of $\sim 10^{12}$ cm^{-3} (Fig. 4) to $\sim 10^{13}$ cm^{-3} (Fig. 7) for the WE diodes.

The other two hole traps H2 and H3 in Fig. 5 give rise to an activation enthalpy of 0.29 eV and 0.415 eV, respectively. It should first of all be remarked that there is a rather large error bar on the extracted values, given the rather noisy and broad character of the small peaks. Nevertheless, we may compare with other Ni-[36] and Cu-related[37,38] deep levels found in the literature in the same temperature range. The H2 hole trap is close to the H150 level at E_V+0.29 eV and assigned to a Ni-H related defect.[36] For H3, two possible candidates could be the H190 Ni-H_2 single acceptor at E_V+0.46 eV or the H240 Ni-H (+/0) single donor level at E_V+0.49 eV.[36] From forward-bias stressing the n^+p diodes, it was derived that the active B concentration in the depletion region can be reduced, suggesting the passivation by mobile hydrogen.[31] This could provide some support for the presence of Ni-H related hole traps in the p-type depletion region. Quite recently, it has been shown that Cu-Ni related hole traps can be formed in p-type Cu-doped silicon at about 160 and 190 K.[38] However, they appear to be unstable at room temperature, disappearing from detection after two days. It is unlikely that we are observing these levels here, as DLTS has been performed several weeks after processing the devices.

Alternatively, the level at E_V+0.29 eV is close to the interstitial carbon C_i related donor.[39–43] However, as the DLTS measurements have been performed a long time after the solar cell processing and considering the high diffusivity and reactivity of C_i at room temperature, this assignment is rather unlikely. Another possible candidate could be the B_i-B_s level at E_V+0.28 eV found in 10 MeV proton-irradiated p-type solar cells.[44] The origin of level H3 appears to be even more obscure – one possibility could be the unidentified level at E_V+0.40 eV in carbon-implanted p-type silicon.[40]

Filling of the H1 trap by holes is investigated in function of the pulse duration t_p in Fig. 6 for a wet-etched n^+p diode, at different temperatures. It can be derived from this plot that trap filling occurs between 10 μs and 1 ms in the T-range of 90 K to 95.8 K. It means that a t_p of 1 ms is sufficient to saturate the trap concentration in Fig. 4 for peak H1. At the same time, similar filling rates can be observed, indicating a weak temperature dependence of the hole capture cross section in this case.

The use of a n^+p junction allows to inject minority carriers in the p-type base during a bias pulse into forward operation, enabling the detection of minority carrier (electron) traps in the upper half of the bandgap.[32,33] Figure 7 compares the majority carrier spectra with a minority carrier injection curve, for a pulse from −1 V to +0.7 V for a WE diode. During the forward-bias pulse, minority electrons will be injected close to the junction and are available for capture by electron traps. In this case, a pronounced negative peak at 75 K is observed in Fig. 7. The corresponding shallow electron trap could be the double acceptor level of $Ni_s^{-/2-}$ at E_C-0.07 eV.[36] However, a second, single acceptor peak at E_C-0.45 eV (E_C, the bottom of the conduction band) would be expected, which is not clearly found in Fig. 7. Perhaps the small negative feature around 200 K belongs to this centre. Alternatively, the electron trap could be identified as the acceptor level of C_i or a more stable C-related complex.[42] The origin of the second broad electron trap around 125 K is as yet unclear. In general, the identification of minority carrier traps in DLTS is more challenging.

According to Fig. 8, the standard LA diode exhibits DLT-spectra which are similar to the WE case (Fig. 4). For example, trap H1 is also present, indicating that the nickel-silicidation process most likely introduces nickel in the underlying p-type base, irrespective of the contact opening method. According to Fig. 9, similar activation energies as in Fig. 5 can be derived from an Arrhenius plot for the hole traps H1

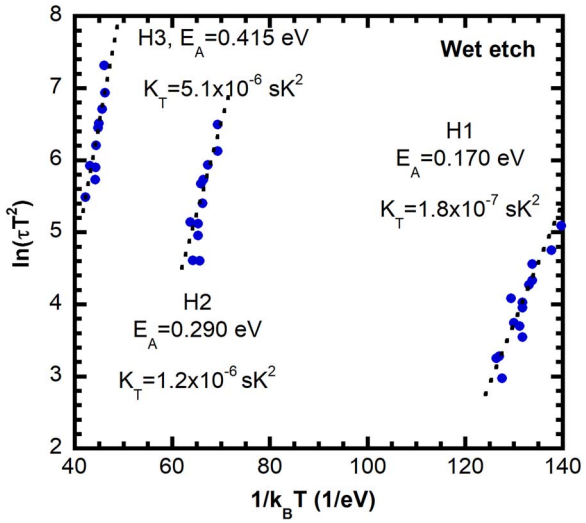

Figure 5. Arrhenius plot for the hole traps H1, H2 and H3 observed by DLTS in the p-type base region. k_B is Boltzmann's constant.

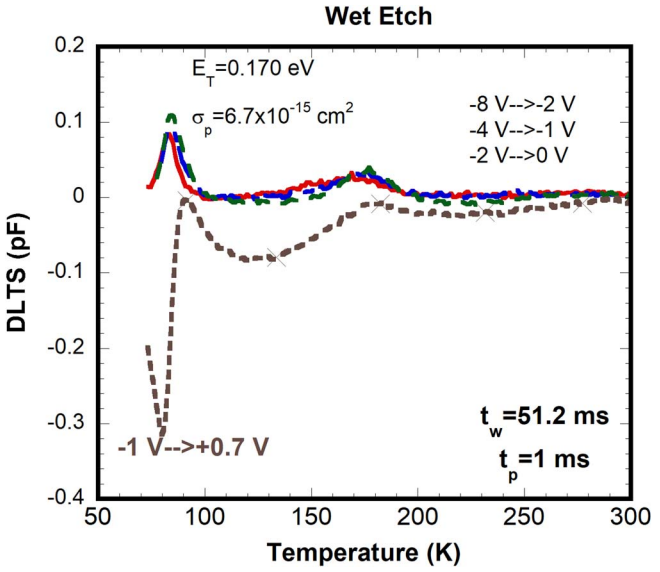

Figure 7. Forward injection spectrum for a pulse from −1 V to +0.7 V, compared with the majority carrier spectra for a wet-etched n^+p diode.

and H2 in the standard LA diode. Also the trap concentrations N_T are on the same order of magnitude, in the range of 10^{13} cm^{-3}, considering a p-type doping concentration of 2×10^{16} cm^{-3}. Finally, the trap filling by holes exhibits the same kinetics as evidenced by Fig. 10, in comparison with Fig. 6.

The hard LA sample equally exhibits the 80 K hole trap in Fig. 11, with a similar peak height, i.e., trap concentration. The level H3 is not clearly detected in the spectrum, while a new hole trap emerges around 175 K. This peak is rather broad, suggesting it does not belong to a simple point defect and changes its position with bias pulse; its peak position moves to higher T for a bias pulse closer to the junction. It indicates that instead of a single level, a density-of-states (DOS) is being probed, possibly associated with extended defects. From previous work, it has been established that under LA conditions, dislocations are formed,[28–30] which at high laser power can penetrate from the emitter into the p-type base. Comparing the broad band in Fig. 11 with literature data for plastically deformed p-type silicon, similar broad peaks

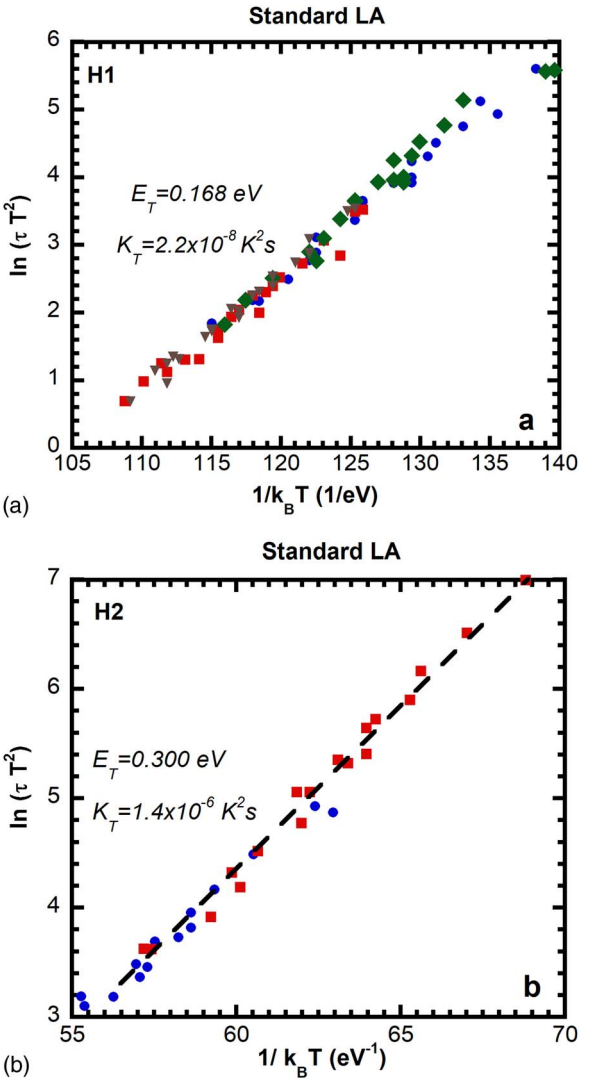

Figure 9. Arrhenius plot for a standard LA n^+p junction and corresponding with hole trap H1 (a) and H2 (b). The data points has been extracted from spectra corresponding with different pulses.

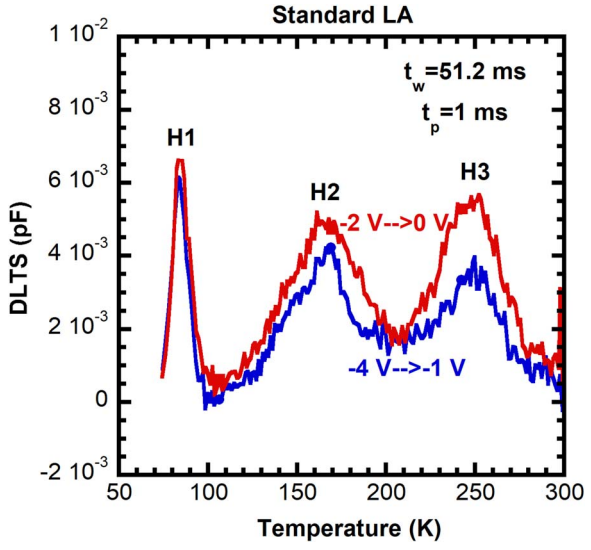

Figure 8. DLT-spectra for different bias pulses, using a sampling time constant $t_w = 51.2$ ms and a pulse duration $t_p = 1$ ms for a standard laser-ablated n^+p diode.

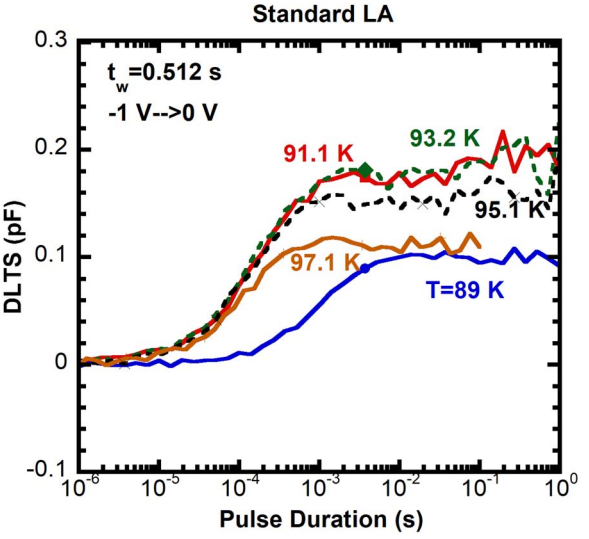

Figure 10. DLTS amplitude versus pulse duration for the H1 peak in a standard LA n^+p junction, corresponding with different measurement temperatures and a sampling period $t_w = 0.512$ s. The pulse was from −1 V to 0 V.

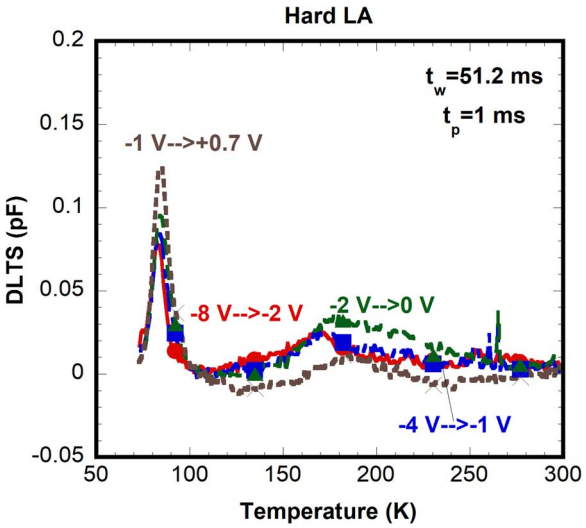

Figure 11. DLT-spectra for different bias pulses, using a sampling time constant $t_w = 51.2$ ms and a pulse duration $t_p = 1$ ms for a hard laser-ablated n^+p diode.

have been found in the range of $E_V+0.4$ eV to $E_V+0.5$ eV.[45–49] In this case, no clear minority carrier peaks have been found in the -1 V to $+0.7$ V spectrum.

A further way to confirm the extended defect nature of the traps in the hard LA diode is by recording the trap filling kinetics.[49] Figure 12 shows the evolution of the spectra as a function of the pulse duration t_p. While there is no pronounced evolution of the 175 K band, surprisingly, a pronounced increase of the peak amplitude with t_p is observed for the 80 K level. The trap filling in the range from 100 µs to 10 ms does not saturate, in contrast to the behavior for the WE (Fig. 6) and standard LA diode (Fig. 10), where a constant peak amplitude is found in that t_p range. It indicates a major change in the capture kinetics, which could be understood in terms of a change in the hole capture cross section (with temperature) or in a change of the free hole density. The peak amplitude keeps increasing and resembles more what is expected for an extended defect, like a dislocation, namely, a trap filling increasing proportionally with $\ln(t_p)$. This casts some doubt on the assignment of the H1 level in the hard LA diodes to a point defect, and more specific

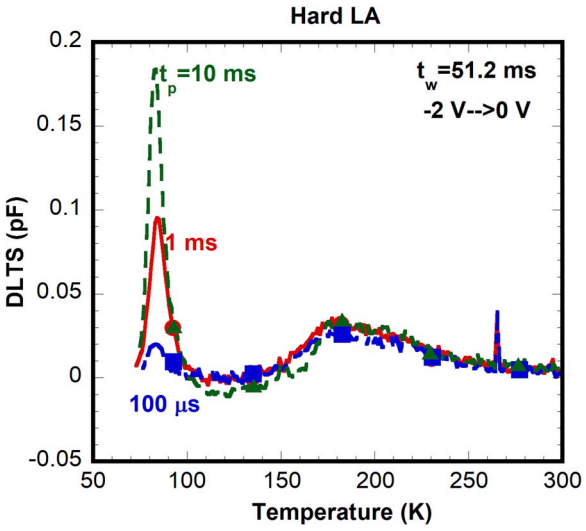

Figure 12. DLT-spectra for a hard LA n^+p diode, using a pulse from -2 V to 0 V corresponding with different pulse durations. The sampling period is 51.2 ms.

to the donor level of Ni_s. Moreover, the capture kinetics is much slower than would be expected for a level with a hole capture cross section of 7×10^{-15} cm^2. Considering a doping density of 2×10^{16} cm^{-3}, one expects a capture time constant in the range of 10 µs – much faster than observed in Fig. 12.

One could associate the 80 K peak in Fig. 11 with some shallow dislocation-related hole traps.[47,48] The fact that the same level is present in WE samples contradicts this interpretation, as no dislocations are expected to occur in that case. A tentative alternative model is to assume that the hole trap still corresponds with a point defect, but occurring in the strain field of a dislocation. In other words, the point defects decorate the dislocations and are affected by the repulsive potential barrier with height $q\Phi$ existing around a charged dislocation and repelling majority carriers. This causes a slower than expected trap filling, with a corresponding hole concentration profile given by $p_0\exp(-q\Phi/k_BT)$, with p_0 the free carrier concentration outside the space charge cylinder surrounding a dislocation. In fact, a similar observation has been found in the past for Fe atoms decorating dislocations in p-type silicon.[50]

Summary

Deep levels in silicon n^+p solar cells with copper metallization have been studied for different contact opening methods, either based on a standard wet etching or on laser ablation. A hole trap at 0.17 eV from the valence band is found consistently in all samples, irrespective of the contact opening and is tentatively assigned to the donor level of substitutional nickel. Deeper hole traps are found as well, which depend on the processing conditions: while two more types of point defects are found for the WE and standard LA diode, one single broad band is found for the hard LA samples, which could be associated with dislocations formed during the contact opening and penetrating from the shallow emitter into the p-type base.

Acknowledgments

The authors would like to thank R. Russell for plating the p-PERC solar cells in this study, as well as L. Tous and M. Recaman for assistance with processing and discussion. The support of the characterization group is also deeply acknowledged.

ORCID

E. Simoen https://orcid.org/0000-0002-5218-4046

References

1. J. Bartsch, A. Mondon, K. Bayer, C. Schetter, M. Hörteis, and S. W. Glunz, *J. Electrochem. Soc.*, **157**, 942 (2010).
2. S. Flynn and A. Lennon, *Solar Energy Mater. & Solar Cells*, **130**, 309 (2014).
3. A. Kraft, C. Wolf, J. Bartsch, and M. Glatthaar, *Energy Procedia*, **67**, 93 (2015).
4. A. A. Istratov, C. Flink, and E. R. Weber, *Phys. Status Solidi B*, **222**, 261 (2000).
5. A. A. Istratov and E. R. Weber, *J. Electrochem. Soc.*, **149**, G21 (2002).
6. M. Itsumi, *Appl. Phys. Lett.*, **63**, 1095 (1993).
7. M. Itsumi, Y. Sato, K. Imai, and N. Yabumoto, *J. Appl. Phys.*, **82**, 3250 (1997).
8. K. Kurita and T. Shingyouji, *Jpn. J. Appl. Phys.*, **37**, 5861 (1998).
9. M. Boehringer, J. Hauber, S. Passefort, and K. Eason, *J. Electrochem. Soc.*, **152**, G1 (2005).
10. H. Savin, M. Yli-Koski, A. Haarahiltunen, N. Talvitie, and J. Sinkkonen, *ECS Trans.*, **11**(3), 319 (2007).
11. R. H. Hopkins, S. G. Seidensticker, J. R. Davis Jr, O. Rai-Choudhury, P. D. Blais, and J. R. McCormick, *J. Cryst. Growth*, **41**, 493 (1977).
12. J. R. Davis Jr., A. Rohatgi, R. H. Hopkins, P. D. Blais, P. Rai-Choudhury, J. R. McCormick, and H. C. Mollenkopf, *IEEE Trans. Electron Devices*, ED-**27**, 677 (1980).
13. R. H. Hopkins and A. Rohatgi, *J. Cryst. Growth*, **75**, 67 (1986).
14. M. L. Polignano, D. Caputo, C. Carpanese, G. Salvà, and L. Vanzetti, *Eur. Phys. J. Appl. Phys.*, **27**, 435 (2004).
15. A. A. Istratov, H. Hedemann, M. Seibt, O. F. Vyvenko, W. Schröter, T. Heiser, C. Flink, H. Hieslmair, and E. R. Weber, *J. Electrochem. Soc.*, **145**, 3889 (1998).
16. W. B. Henley, D. A. Ramappa, and L. Jastrzebski, *Appl. Phys. Lett.*, **74**, 278 (1999).
17. D. A. Ramappa, *Appl. Phys. Lett.*, **76**, 3756 (2000).
18. A. A. Istratov, H. Hieslmair, and E. R. Weber, *Appl. Phys. A*, **70**, 489 (2000).

19. H. Vahlman, A. Haarahiltunen, W. Kwapil, J. Schön, A. Inglese, and H. Savin, *J. Appl. Phys.*, **121**, 195704 (2017).
20. D. Graff, *Metal Impurities in Silicon-Device Fabrication*, Springer, Heidelberg, Germany (2000).
21. M. L. Polignano, F. Cazzaniga, A. Sabbadini, G. Queirolo, A. Cacciato, and A. Di Bartolo, *Mat. Sci. Eng. B*, **42**, 157 (1996).
22. W. Wang, Z. Xi, D. Yang, and D. Que, *Mater. Sci. Semicond. Process.*, **9**, 296 (2006).
23. M. L. Polignano, D. Codegoni, S. Grasso, A. Riva, F. Sammiceli, D. Caputo, and V. Privitera, *ECS Trans.*, **16**(6), 195 (2008).
24. Y. Yoon, B. Paudyal, K. Kim, Y.-W. Ok, P. Kulshreshtha, S. Johnston, and G. Rozgonyi, *J. Appl. Phys.*, **111**, 033702 (2012).
25. M. Seibt, D. Abdelbarey, V. Kveder, C. Rudolf, P. Saring, L. Stolze, and O. Voß, *Phys. Status Solidi C*, **6**, 1847 (2009).
26. M. Tsuchiaki, K. Ohuchi, and C. Hongo, *Jpn. J. Appl. Phys.*, **43**, 5166 (2004).
27. M. Tsuchiaki and A. Nishiyama, *Jpn. J. Appl. Phys.*, **46**, 1830 (2007).
28. Z. Sun and M. C. Gupta, *J. Appl. Phys.*, **124**, 223103 (2018).
29. Y. Weng, B. Kedjar, K. Ohmer, J. R. Köhler, J. H. Werner, and H. P. Strunk, *Phys. Status Solidi C*, **10**, 28 (2013).
30. C. Dang, R. Labie, L. Tous, R. Russell, M. Recaman, J. Deckers, A. Uruena, F. Duerinckx, and J. Poortmans, *Energy Procedia*, **55**, 649 (2014).
31. C. Dang Thuy, unpublished results.
32. E. Simoen, J. Lauwaert, and H. Vrielinck, *Semiconductors, and Semimetals*, 91, Eds L. Romano, V. Privitera, and C. Jagadish, 205, (2015).
33. A. R. Peaker, V. P. Markevich, and J. Coutinho, *J. Appl. Phys.*, **123**, 161559 (2018).
34. C. Dang, R. Labie, E. Simoen, L. Tous, R. Russell, F. Duerinckx, R. Mertens, and J. Poortmans, *Proc. of SiPV 2017, Energy Procedia*, **124**, 862 (2017).
35. C. Dang, R. Labie, E. Simoen, F. Duerinckx, and J. Poortmans, *Solar Energy Materials and Solar Cells*, **184**, 57 (2018).
36. L. Scheffler, Vl. Kolkovsky, and J. Weber, *J. Appl. Phys*, **116**, 173704 (2014).
37. S. Knack, *Mater. Sci. in Semicond. Process.*, **7**, 125 (2004).
38. N. Yarikin and J. Weber, *Phys. Status Solidi A*, 1900304 (2019).
39. Y. H. Lee, L. J. Cheng, J. D. Gerson, P. M. Mooney, and J. W. Corbett, *Solid St. Commun.*, **21**, 109 (1977).
40. B. N. Mukashev, A. V. Spitsyn, N. Fukuoka, and H. Saito, *Jpn. J. Appl. Phys.*, **21**, 399 (1982).
41. C. A. Londos, *Phys. Rev. B*, **35**, 6295 (1987).
42. M. T. Asom, J. L. Benton, R. Sauer, and L. C. Kimerling, *Appl. Phys. Lett.*, **51**, 256 (1987).
43. G. Ferenczi, C. A. Londos, T. Pavelka, M. Somogyi, and A. Mertens, *J. Appl. Phys.*, **63**, 183 (1988).
44. A. Khan, M. Yamaguchi, Y. Ohshita, N. Dharmarasu, K. Araki, T. Abe, H. Itoh, T. Ohshima, M. Imaizumi, and S. Matsuda, *J. Appl. Phys.*, **90**, 1170 (2001).
45. L. C. Kimerling and J. R. Patel, *Appl. Phys. Lett.*, **34**, 73 (1979).
46. O. V. Feklisova, B. Pichaud, and E. B. Yakimov, *Phys. Satus Solidi A*, **202**, 896 (2005).
47. D. Cavalcoli and A. Cavallini, *Phys. Status Solidi C*, **4**, 2871 (2007).
48. D. Cavalcoli, A. Castaldini, and A. Cavallini, *Appl. Phys. A*, **90**, 619 (2008).
49. W. Schröter and H. Cerva, *Solid. St. Phenom.*, **85–86**, 67 (2002).
50. R. Khalil, V. Kveder, W. Schröter, and M. Seibt, *Phys. Status Solidi C*, **2**, 1802 (2005).